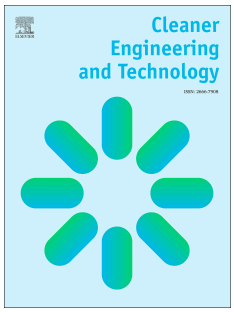

Effect of mining residues treated with an electrodialytic technology on cement-based mortars

J. Almeida, P. Faria, A.B. Ribeiro, A. Santos Silva

PII: S2666-7908(20)30001-X

DOI: https://doi.org/10.1016/j.clet.2020.100001

Reference: CLET 100001

To appear in: *Cleaner Engineering and Technology*

Received Date: 3 July 2020

Revised Date: 12 August 2020

Accepted Date: 5 September 2020

Please cite this article as: Almeida, J., Faria, P., Ribeiro, A.B., Silva, A.S., Effect of mining residues treated with an electrodialytic technology on cement-based mortars, *Cleaner Engineering and Technology*, https://doi.org/10.1016/j.clet.2020.100001.

Effect of mining residues treated with an electrodialytic technology on cement-based mortars

J. Almeida[1,2]*, P. Faria[1,3*], A. B. Ribeiro[2] and A. Santos Silva[4]

[1] Department of Civil Engineering, NOVA School of Sciences and Technology, NOVA University of Lisbon, 2829-516 Caparica, Portugal

[2] CENSE, Department of Sciences and Environmental Engineering, NOVA School of Sciences and Technology, NOVA University of Lisbon, 2829-516 Caparica, Portugal

[3] CERIS and Department of Civil Engineering, NOVA School of Sciences and Technology, NOVA University of Lisbon, 2829-516 Caparica, Portugal

[4] Materials Department, National Laboratory of Civil Engineering, 1700-066 Lisbon, Portugal

*Corresponding authors.

E-mail addresses: js.almeida@campus.fct.unl.pt (J. Almeida); paulina.faria@fct.unl.pt (P. Faria)

Mining residues

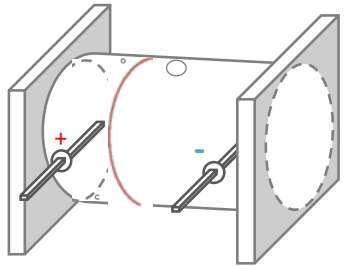

Electrodialytic treatment

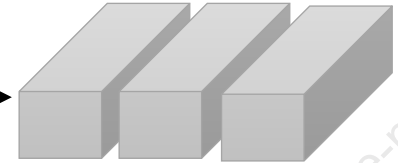

Cement-based mortars

10, 25 & 50% cement replacement

28 day-curing

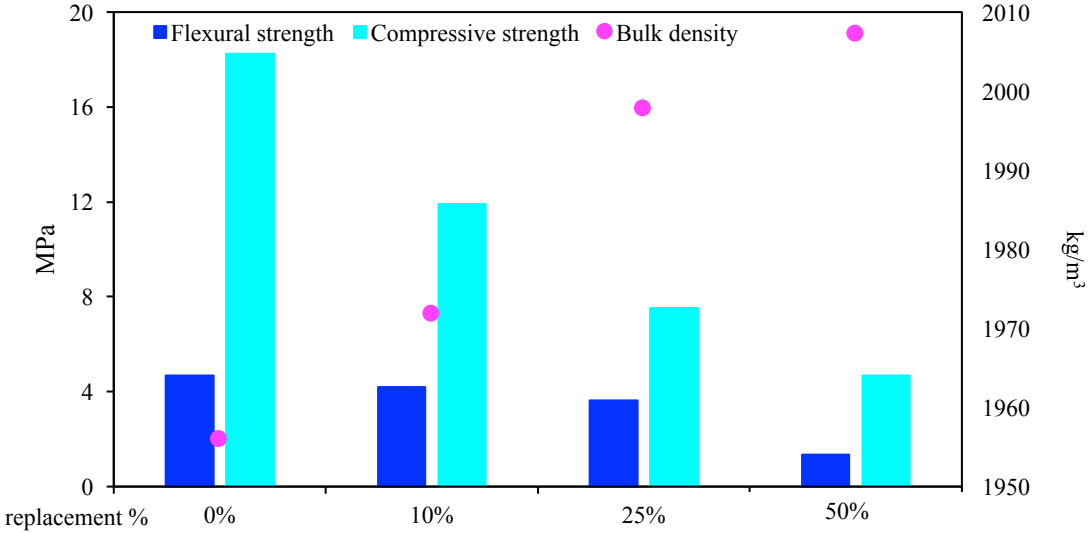

Classification					
	Rendering (EN 998-1)	CS IV	CS IV	CS III	CS III
	Masonry (EN 998-2)	M15	M10	M10	M5

Effect of mining residues treated with an electrodialytic technology on cement-based mortars

J. Almeida[1,2]*, P. Faria[1,3*], A. B. Ribeiro[2] and A. Santos Silva[4]

[1] Department of Civil Engineering, NOVA School of Sciences and Technology, NOVA University of Lisbon, 2829-516 Caparica, Portugal

[2] CENSE, Department of Sciences and Environmental Engineering, NOVA School of Sciences and Technology, NOVA University of Lisbon, 2829-516 Caparica, Portugal

[3] CERIS and Department of Civil Engineering, NOVA School of Sciences and Technology, NOVA University of Lisbon, 2829-516 Caparica, Portugal

[4] Materials Department, National Laboratory of Civil Engineering, 1700-066 Lisbon, Portugal

*Corresponding authors.

E-mail addresses: js.almeida@campus.fct.unl.pt (J. Almeida); paulina.faria@fct.unl.pt (P. Faria)

Highlights

- Mining residues were electrodialytic treated (ED) to extract raw materials
- Raw and ED mining residues replaced cement in 10, 25 and 50 % (volume) in mortars
- Mechanical strength of modified mortars decreased between 11 and 30 %
- Water absorption increased although drying capacity of modified mortars was improved
- ED mining residues are viable mortar materials for masonry, rendering and screeds

Abstract

Mining residues have been accumulated for centuries due to excavation and mining processes, causing environmental degradation worldwide. Their application in cementitious products is a feasible alternative to waste disposal. Electrodialytic technologies can promote a safer reuse of mining residues in the construction sector, coupling economic advantages due to the possible removal of toxic elements and the recovery of critical raw materials. The application of treated mining residues in construction products, namely their effects on physico-mechanical properties, in comparison to raw residues and cement uses needs to be addressed. This work presents a study of cement-based mortars with the incorporation of mining residues treated with an electrodialytic process in comparison to raw mining residues. The replacement percentages studied were 0, 10, 25 and 50 % of the binder in volume. Tests

were conducted to evaluate fresh and hardened properties of mortars considering physical, microstructural and mechanical performances. Results show the viability of applying mining residues after the electrodialytic treatment as mortars materials in rendering, plastering, joint repointing, bedding masonry or screed requirements, with improved thermal conductivity and eco-efficiency.

Keywords

Cement composite; construction product; electrodialytic process; mining residue; masonry mortar

Abbreviations

Cac - capillarity absorption coefficient

$Ca(OH)_2$ - calcium hydroxide

CEN - European Committee for Standardization

Cs - capillarity saturation value

CStr - compressive strength

DI - drying index

DME - dynamic modulus of elasticity

DR1 - drying rate at phase 1

DR2 - drying rate at phase 2

ED - electrodlialytic process

FStr - Flexural strength

M - raw mining residues mortars

ME - electrodialytic treated mining residues mortars

MIP - mercury intrusion porosimetry

$NaNO_3$ - sodium nitrate

OPC - ordinary Portland cement

REF - reference mortar

RH - relative humidity

Ti/MMO - titanium/mixed metal oxide

XRF - X-ray fluorescence

WO_3 - tungsten trioxide

1. Introduction

The sustainable progress of the planet is highly dependent on global population trends. Since the world population is expected to reach 10.9 billion by 2100 (from current 7.7 billion), urban areas will face serious challenges in its sustainable development (United Nations, 2019).

Concrete is one of the main contributors for greenhouse gas emissions and its manufacture commonly involves Portland cement binders, likewise Portland cement-based mortar production (Arrigoni et al., 2020). Mortars are porous construction composites frequently used for bedding masonry units, plastering, rendering and for screeds (Faria et al., 2015). The performance of mortars depends on the properties of the materials involved, their proportions, production and application procedures and curing conditions (Shi et al., 2020). Typically, masonry bedding mortars require higher compressive strength when compared to plastering and rendering mortars; in turn the latter implies low shrinkage and rigidity, and high workability and flexural resistance (Di Mundo et al., 2020).

Focusing on rendering mortars maintenance, mortar components and application may affect renders' durability, the need for repair interventions and the overall construction sustainability. Cement-based mortars may have higher impacts in the beginning of their life cycle, but these negative impacts generally decrease overtime, mainly due to a reduced need for repair actions in comparison with non-hydraulic mortars (Brás and Faria, 2017). Renders main function is to protect walls where they are applied. Thus, cementitious renders are compatible with concrete monolithic walls, concrete block or fired brick masonry walls (Palomar et al., 2019).

Under circular economy targets, alternative secondary resources are highly encouraged for different purposes (EC, 2020). Thus, research has focused in the development of sustainable cementitious products to minimize the negative impacts associated to ordinary Portland cement (OPC). A partial replacement by alternative secondary resources may bring economic, social and environment benefits, as well as an improvement on durability properties (Li et al., 2020).

During the past decades, mineral exploitation has gained an international demand due to the global economic growth. In Europe, Portugal is one of the main producers of copper and tungsten concentrates at Neves Corvo mine (Capasso et al., 2019) and Panasqueira mine (Almeida et al., 2020b), respectively.

Mining processes are associated to a critical environmental problem worldwide due to their high waste disposal rates. Generally, metal mining generates approximately 15 billion tonnes

of waste per year, which is 10 times more than global municipal waste (Gankhuyag and Gregoire, 2018). This waste can affect the ecosystems due to their: (1) chemical and mineralogical composition; (2) physical properties; (3) volume and surface occupied and (4) waste disposal method. Mining residues are often disposed in large areas with dumps or in abandoned open pits. The most common management approaches are, thus, terrestrial impoundment, underground backfilling, deep water disposal and recycling. In this sense, the main risks associated are the failure of mining waste disposal dams and the dispersion of waste fines and heap leaching (Lèbre et al., 2017).

Regarding Panasqueira mine (Covilhã, Portugal) several researches focused on tungsten mining residues reuse in construction products. Some examples are alkali activated products (Beghoura and Castro-Gomes, 2019; Sedira et al., 2018), technical-artistic value added products (Castro-Gomes et al., 2012) and pozzolanic materials (Sousa et al., 2013) that, alone or coupled with other resources, may improve the properties of construction products.

The presence of valuable raw materials and harmful compounds in these secondary resources have pursued the development of new approaches to promote its safe further reuse, namely in the construction sector (Almeida et al., 2020b).

The electrodialytic process (ED) consists on the application of a low-level alternate/direct current density between pairs of electrodes to remove organic and inorganic substances. Ion exchange membranes are used to promote a selective separation of anions and cations in concentrated salty solutions (Ribeiro and Rodríguez-Maroto, 2006). This treatment is commonly applied to liquid [e.g. effluent (Magro et al., 2019)] or solid [e.g. soil (Guedes et al., 2014), sewage sludge (Guedes et al., 2016), fly ash (Magro et al., 2016), timber waste (Ribeiro et al., 2000)] matrices. In particular, ED has shown potential not only to promote the removal of toxic elements or the recovery of critical raw materials but also to enhance properties of tungsten mining residues in the presence of natural adjuvants (Almeida et al., 2020a), namely composites durability (Almeida et al., 2020c). However, to the authors knowledge, the effect of ED treated mining residues in comparison to raw mining residues applications in construction products properties has not yet been studied.

The present work aims to show the feasibility of using secondary mining resources in cement-mortars production as binder replacement, after being treated with an ED process. By the application of the ED pre-treatment, this novel procedure contributes to increase critical raw materials recovery (e.g. tungsten), and harmful compounds removal (e.g. arsenic) from mining residues suspensions, promoting a cleaner reuse of this secondary resource in cement composites. Also, this study contributes for a secondary resource reuse approach towards

circular economy principles. The present research gives an overview on fresh and hardened properties of the mortars produced with 0, 10, 25 and 50 % of cement content replacement (in volume) by raw or treated mining residues in order to access the feasibility of applying the ED technology without materials deterioration when compared to raw residues uses.

2. Experimental campaign

2.1 Materials

Mortars were produced with tungsten mining mud collected directly from the sludge circuit output of Panasqueira mine (Covilhã, Portugal, 40°10′11″N, 7°45′24″W). Samples were dried at 20 ºC for 48 h in a fume hood, before starting the experiments. Typically, mud from Panasqueira mine contains fines with particle sizes lower than 2 mm (Castro-Gomes et al., 2011). The annual production of tungsten at Panasqueira mine is estimated in 90,000 t, with concentrated grades of 75 % WO_3 (tungsten trioxide) (Franco et al., 2014).

In this work, tungsten mining residues were applied as replacement of CEM II/BL 32.5 N (Secil, Portugal), classified according to EN 197-1 (CEN, 2012). A river siliceous sand was applied as aggregate and tap water was used to hydrate the formulation.

2.2 Methods

2.2.1. Electrodialytic treatment of mining residues

The ED treatment was applied for the recovery of critical raw materials (tungsten), and the removal of harmful compounds (arsenic) from mining residues (Almeida et al., 2020a).

Mining residues were treated in a two-compartment ED acryl XT reactor (RIAS A/S, Roskilde, Denmark), according to Almeida et al. (2020a). The diameter of the reactor was 80 mm, with 50 mm length for the electrolyte compartment and 100 mm for the sample section. An anion exchange membrane AR204SZRA, MKIII, Blank (Ionics, USA) was applied to divide the two compartments. The electrodes selected were made of Ti/MMO with a length of 50 mm and a diameter of 3 mm (Grønvold & Karnov A/S, Denmark). Constant current was maintained inside the reactor (50 mA) with a power supply E3612A (Hewlett Packard, Palo Alto, USA).

Also, a magnetic stirrer was placed into the sample compartment. A suspension of 39 g of mining residues with 345 mL of deionized water and 5 mL of a natural deep eutectic solvent (choline chloride/malonic acid) was set in the cathode compartment. In the anode

compartment, 250 mL of 0.01 M $NaNO_3$ were added as anolyte. Twenty experiments were operated during 4 days.

2.2.2 Materials' properties

The particle size distribution of the river siliceous sand was performed by dry sieving following standard EN 1015-1 (CEN, 1998). Loose bulk density of CEM II/BL 32.5 N, river sand, raw mining residues and ED mining residues was determined weighting a recipient with known volume filled with each uncompacted material. The chemical composition of the raw and ED mining residues was determined with a portable X-ray fluorescence equipment (XRF), Tracer 5 from Bruker.

2.2.3 Mortar formulation, samples curing and tests

The production of mortars (type, velocity and time of mixing) was carried out based on EN 196-1 (CEN, 2017). The volumetric proportion of binder, aggregate and water used as reference was 1:3:0.5. The reference mortar was produced with 100 % of CEM II/BL 32.5 N as binder. Modified mortars were produced replacing 10, 25 and 50 % of the cement volume content by raw (M mortars) and ED (ME mortars) mining residues. The loose bulk density of the materials allowed to determine the exact masses of each component, considering their volumes (Table 1).

Table 1. Weight proportion of binder, aggregate and water used in the mortar formulations, materials loose bulk density and water/binder mass ratio.

	Binder and mining residues					**Aggregate**		**Water**		**Mass proportion**	
	CEM II/BL 32.5 N (1000 kg/m^3)		Mining residues			Sand (1540 kg/m^3)		Tap water (1000 kg/m^3)		Binder:sand :water	Cement:residue:sand
Code	%	Weight (g)	Treatment	%	Weight (g)	%	Weight (g)	%	Weight (g)		
REF	100	431.8	-	-	-					1:4.6:0.8	1:0:4.6
M10	90	388.7	No treatment (M) (1180 kg/m^3)	10	36.6					1:4.7:0.8	1:0.1:5.1
M25	75	323.9		25	91.4					1:4.8:0.8	1:0.3:6.2
M50	50	215.9		50	182.9	100	2000	100	333.3	1:5.0:0.8	1:0.9:9.3
ME10	90	388.7	Electrodialytic treated (ME) (1003 kg/m^3)	10	42.0					1:4.6:0.8	1:0.1:5.1
ME25	75	323.9		25	105.0					1:4.7:0.8	1:0.3:6.2
ME50	50	215.9		50	209.9					1:4.7:0.8	1:1.0:9.3

Notation: REF - Reference mortar; M - Raw mining residues mortars; ME – Electrodialytic treated mining residues mortars.

Mortars' fresh and hardened state properties were analysed through physical, mechanical and microstructural tests, as summed up in Figure 1.

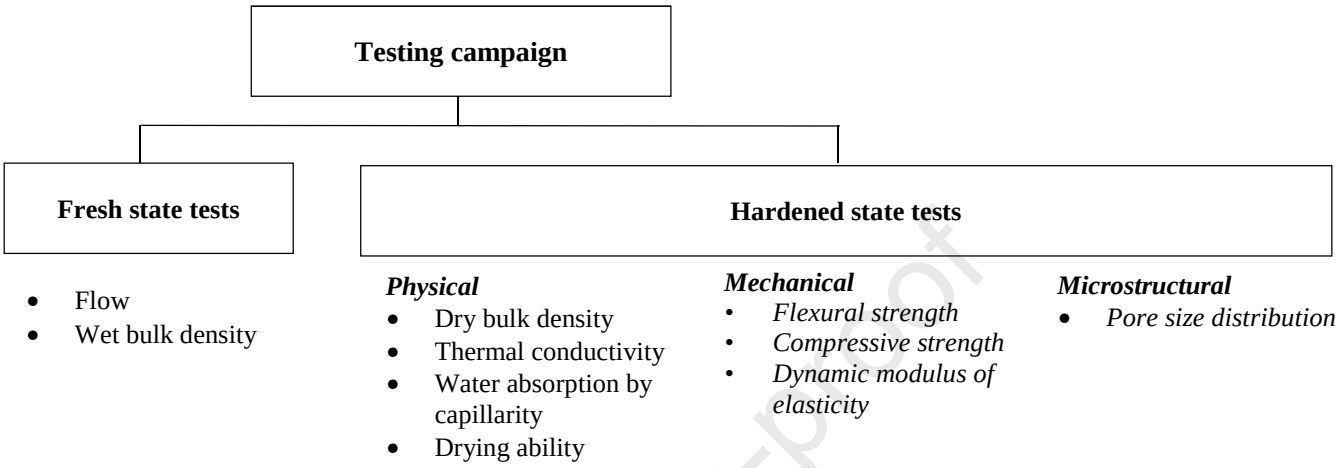

Figure 1. Tests performed to assess fresh and hardened mortars properties.

Flow consistency tests were performed according to EN 1015-3 (CEN, 2000). A flow table test was used to measure the slump value (average diameter of the specimen measured in different directions). Bulk density of fresh mortars was determined according to EN 1015-6 (CEN, 1999a) by weighting a mould (with known volume) filled with the mortar specimen.

Mortar samples were produced in triplicate in 40 mm x 40 mm x 160 mm metallic moulds. For each mortar formulation, circular samples with 90 mm diameter and 20 mm width were also produced. Mortar samples were kept inside polyethylene closed bags and demoulding was carried out after 48 h. The samples were cured horizontally in a tap water bath for the next 26 consecutive days at 20 ºC. The samples were then dried at 60 ºC until constant weight.

For thermal conductivity measurements, the circular samples were stabilized in a chamber for 24 h at 20 ^{o}C and 75 % of relative humidity (RH). Thermal conductivity of all specimens was determined inside the chamber with an Isomet 2104 Heat Transfer Analyzer (Applied Precision, Slovakia), equipped with a contact probe API 210412 of 60 mm diameter and operating range between 0.04 and 0.3 W/(m.k).

The dry bulk density of the mortar prisms was determined by the quotient of the mass, with a digital scale (precision of 0.001 g), by the volume, assessed directly with a digital caliper (precision 0.01 mm), based on EN 1015-10/A1 (CEN, 1999b).

The dynamic modulus of elasticity (DME) was determined considering EN 14146 (CEN, 2004), using a Zeus Resonance Meter ZMR 001 equipment. With mass and volume data of each sample, the equipment measured the response to an induced vibration signal along the test samples. For each sample, four nondestructive tests were performed, resulting on twelve tests by mortar.

Flexural and compressive strengths were performed according to EN 1015-11 (CEN, 2019), with a Zwick/Rowell Z050 equipment. For flexural strength tests, three-point bending test was performed with two steel supporting rollers separated by 100 mm. The loading was gradually applied at a constant rate of 50 ± 10 N/s until failure occurred. Compressive strength tests were subsequently performed with one of the half samples disjointed in the previous flexure tests. The loading was progressively applied at a constant ratio of 2400 ± 200 N/s until mortar failure.

Capillarity absorption test, based on EN 1015-18 (CEN, 2003), and drying test, based on EN 16322 (CEN, 2013), were performed in a conditioned laboratory at temperature of 20 ^{o}C and 65 % of RH. Tests were conducted on 40 mm cubic samples, cut from halves of previous flexural tests original prisms. The lateral faces were waterproofed by painting with Sikagard 570 W (Sika, Portugal). Samples were placed into a plastic box and the cut surface was maintained in contact with water to a level of 5 mm.

The capillarity absorption curve of mortar samples, in mass increase per area in contact with water by square root of time, was determined by weighing the samples sequentially until an asymptotic value was obtained. The capillarity coefficient was determined using the mass of water absorbed per unit area and square roof of time between 10 and 30 min (initial strait segment of the curves).

Drying ability of the mortars was tested immediately after capillarity tests, moving the cubic samples to a waterproofed surface, inverting (to promote drying only by the surface previously in contact with water) and weighing the samples sequentially until achieving a constant weight (CEN, 2013). From the mortars drying curve (with the mass decrease per drying area) by time, the drying rate of the first drying phase was determined by the negative slope of the initial segment. From the drying curve by square root of time, the second drying phase rate was determined by the negative slope of the intermediate linear segment. The drying index (DI) was also calculated based on equation 1, from EN 16322 (CEN, 2013):

$$DI = \int_{ti}^{t_f} \frac{M_t dt}{M_{max} t_f} \qquad (1)$$

where t_f is the total duration of the test, M_t is the water content in time t, and M_{max} is the maximum water content. A lower DI corresponds to a higher drying capacity.

A mercury porosimeter Micromeritics Autopore II was used to determine pore size distribution from mortars produced with 0, 10, 25 and 50 % of raw mining residues. Specimens with approximately 1.7 cm^3 (total capacity of the bulb from penetrometers) were collected from samples and stabilized in an oven at 40 ºC during 24 h.

3. Results and discussion

3.1. Raw materials characterisation

The chemical composition obtained by XRF of raw and ED mining residues is presented in Table 2. The most abundant elements in both samples is silicon, expressed as SiO_2 (up to 65 %), followed by aluminium, expressed as Al_2O_3 (raw = 19 % and ED = 22 %). Harmful metalloids were also detected in mining residues, such as As (M = 0.59 %), although 64 % of the As was successfully removed by the ED treatment, decreasing the potential of leaching.

Table 2. Semi-quantitative chemical analysis by XRF of raw and ED mining residues (weight %).

Determinations	**Raw**	**ED**
Al_2O_3	18.80	21.98
SiO_2	68.35	65.58
P	0.15	0.10
S	0.83	0.74
Cl	N.D.	N.D.
K_2O	3.29	4.31
Ca	0.55	0.40
Ti	0.46	0.55
Mn	0.08	0.07
Fe	5.81	5.37
Cu	0.18	0.10
Zn	0.58	0.29
As	0.59	0.21
Sn	0.07	0.04
W	0.27	0.26

Notation: N.D. – Not detected.

The loose bulk density of the components used for mortar formulation is presented in Table 1. When mining residues were subjected to the ED treatment, their loose bulk density decreased 15 % compared to the raw case (1180 kg/m^3), which might be due to the extraction

of inorganic substances during the process (Almeida et al., 2020a). Additionally, after the ED treatment of mining residues, their loose bulk density (1003 kg/m^3) became similar to CEM II/BL 32.5 N (1000 kg/m^3). Therefore, the volumetric replacement of the cement binder by ED mining residues almost corresponds to the same weight. On the other hand, the same volumetric replacement by raw mining residues corresponds to a higher weight. Thus, a higher filler effect is expected (Table 1).

The particle size distribution of the river siliceous sand was analysed (Figure 2). Particles are mainly between 0.5 and 2.0 mm, similarly to the CEN reference sand particle size distribution (CEN, 2017).

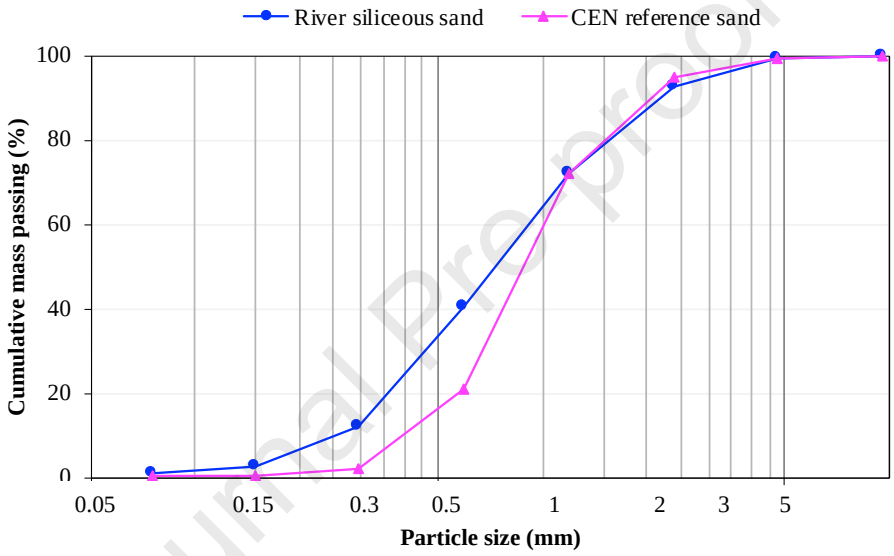

Figure 2. Dry particle size distribution of river siliceous sand and CEN reference sand.

Calcium and aluminium silicates in presence of $Ca(OH)_2$ and water may potentiate a pozzolanic reaction. Mining residues from Panasqueira mine were studied by Almeida et al. (2020c) in terms of its pozzolanic reactivity through the modified Chapelle test (AFNOR, 2010). Herein, the total quantity of fixed $Ca(OH)_2$ by siliceous/aluminosilicates amorphous constituents present in raw and ED mining residues was reported as 7.9 mg and 71.4 mg per g of material, respectively (Almeida et al., 2020c), representing low pozzolanic features.

3.2. Fresh state characterisation

The ability to mix and apply a mortar with minimal loss of homogeneity can be assessed by the fresh state characterisation (Chindaprasirt and Cao, 2015). In this study all the mortars

were produced with a constant water content (Table 1). Concerning the fresh state characterisation, flow table consistency and wet bulk density were determined (Table 3).

Wet bulk density of M and ME showed higher values when compared to the reference mortar, increasing as the content of mining residues augmented in the formulations. Since the loose bulk density of the raw mining residues is higher than cement (Table 1), it was expected that wet bulk density of M mortars was also higher. However, differences on the mortars with ED mining residues, that have similar loose bulk density to cement, were observed.

Table 3. Mortars wet bulk density and flow table consistency.

Mortar	Flow table consistency (mm)	Wet bulk density (kg/m^3)
REF	156.3	1997.9
M10	154.3	2018.7
M25	147.8	2035.2
M50	139.5	2038.2
ME10	146.5	2029.2
ME25	132.3	2038.7
ME50	129.3	2069.8

Notation: REF - Reference mortar; M - Raw mining residues mortars; ME - Electrodialytic treated mining residues mortars.

Loose bulk density of the particles and filler effect are the main factors affecting mortar wet bulk density (Jesus et al., 2019). Mining residues have a pH in water suspension of approximately 5, but after the ED treatment, the pH of mining residues suspensions dropped to about 4 (Almeida et al., 2020a). This may have also affected the difference on bulk density between M and ME mortars, since chemical species present in the residues may have solubilized at a slightly lower pH. The application of natural deep eutectic solvents during the ED treatment, as well as other extreme conditions that mining residues were subjected during the four days of ED experiment, may also have contributed for the bulk density increase. Furthermore, direct water uptake from both raw and ED mining residues could justify the values observed.

The inverse trend was verified for flow consistency tests. The consistency test was performed to assess the fluidity and workability of fresh mortars based on the constant water content (Table 1). Considering the results in Table 3, and also the observations during manual handling of mortars, the incorporation of both types of mining residues (raw and ED) decreased their workability. This loss of workability with the increase of mining residues content may be related to mining residues particles, which may absorb more water due to their permeability and surface properties. The increase of mining residues incorporation may

require more water to achieve the same consistency of the reference mortar, also due to cement hydration reactions. The presence of other chemical substances can interfere with water-binder reactions (Tiwari et al., 2014). The addition of mining residues may hinder chemical bonding between hydration products due to their crystalline phases and inert characteristics (Simonsen et al., 2020).

Mortars were produced with the same volumetric ratio and, consequently, equal binder volume contents but slightly different water/binder mass ratios (Table 1). When mining residues are incorporated in the formulation, the water/binder is affected, which may have also decreased the filler effect, namely in mortars M50 and ME50. The higher incorporation of mining residues reduced the plasticity of the mortars (flow table consistency of 139.5 mm for M50, and 129.3 mm for ME50) compared to the reference (flow table consistency = 156.3 mm). In real conditions, depending on the type of mortar application (e.g. screeds, rendering or plastering), the incorporation of a plasticizer as admixture may be needed to fill water requirements and consistency improvements.

3.3. Hardened state characterisation

The mortar samples used to conduct the hardened state characterization are presented on Figure 3.

Figure 3. Mortar samples after 28 curing days (REF - Reference mortar; M - Raw mining residues mortars; ME - Electrodialytic treated mining residues mortars).

3.3.1. Dry bulk density and thermal conductivity

Hardened mortar results of dry bulk density and thermal conductivity after 28 days of cure are presented in Figure 4.

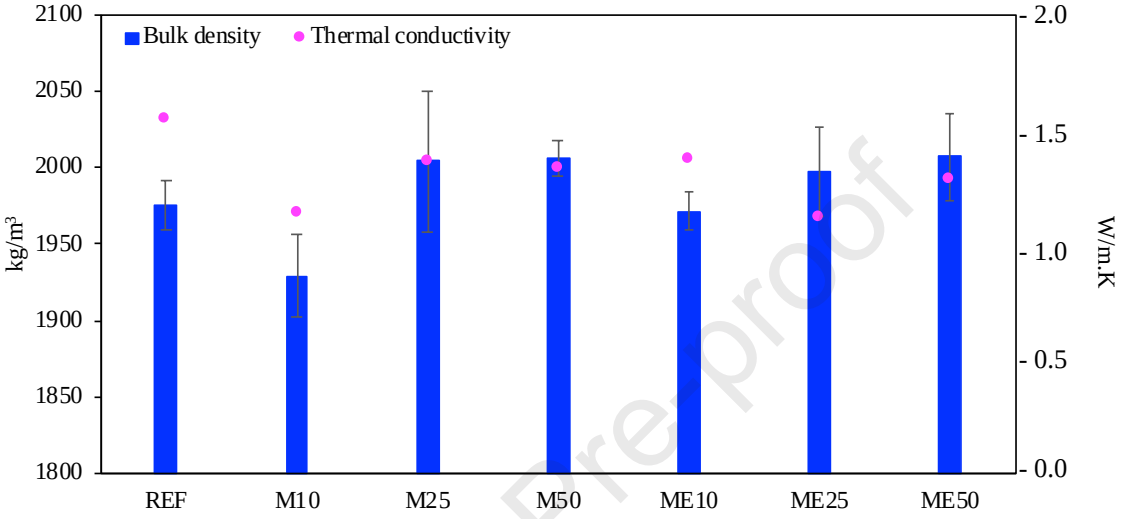

Figure 4. Dry bulk density and thermal conductivity of mortars (REF - Reference mortar; M - Raw mining residues mortars; ME - Electrodialytic treated mining residues mortars).

The trend verified on wet bulk density, with an increase with the content of both mining residues in comparison to the reference, is not observed for the dry bulk density. When 10 % of raw or ED mining residues were introduced in the formulation, dry bulk densities decreased to 1928.9 ± 27.0 kg/m^3 (M10) and 1971.8 ± 12.4 kg/m^3 (ME10) when compared to REF (1975.6 ± 16.8 kg/m^3). However, cement replacement of 25 and 50 % for both M and ME increased the dry bulk density of the mortar by 1-2 % compared to REF, as verified for wet bulk density. Particularly for raw mining residues, this may be explained by the higher mass proportion (Table 1).

For most building applications, low thermal conductivities contribute for thermal comfort, namely for layering masonry mortars or roof screeds. Additionally, low thermal conductivity is desirable in renders to promote the attenuation of thermal expansion stresses (Van Riessen et al., 2009). The reference mortar presents the highest thermal conductivity, 1.54 W/(m.k), suggesting that mining residues incorporation on mortars can improve thermal comfort.

Considering raw mining residues, the trend observed for dry bulk density is maintained: Mortars with higher dry bulk densities were coupled with higher thermal conductivity values. However, the set of mortars with ED mining residues (ME10, ME25 and ME50) did not corroborate the previous trend. ME25 showed the lowest thermal conductivity, 1.15 W/(m.k). The ED treatment may have enhanced the microstructure of the mortar, with optimal conditions for thermal conductivity reduction at 25 % of mining residues incorporation. Therefore, the ED treatment is feasible in terms of both bulk density and thermal conductivity, considering ED mining residues application on cement mortars.

3.3.2. Mechanical resistance

Figure 5 presents the results of flexural (FStr) and compressive (CStr) strengths, as well as dynamic modulus elasticity (DME).

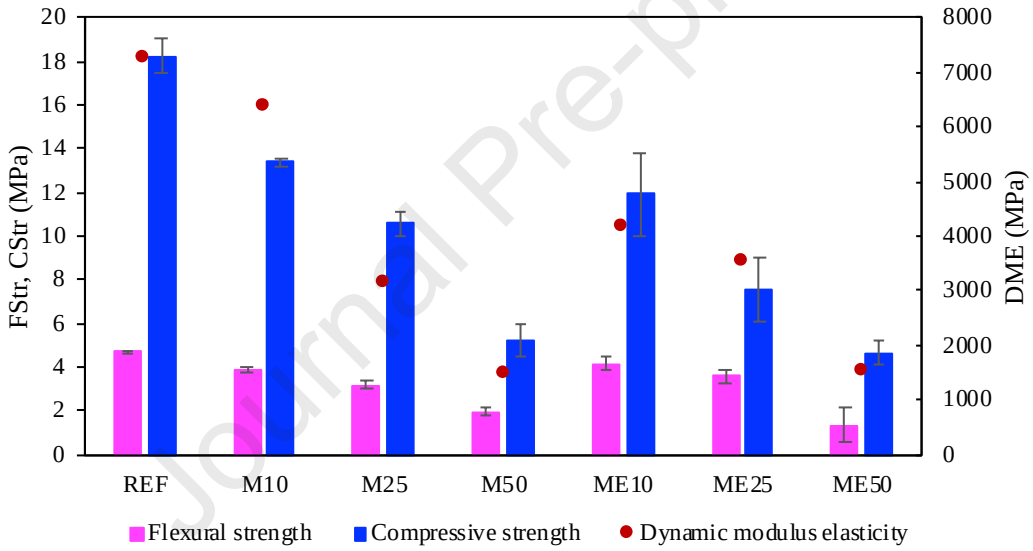

Figure 5. Flexural and compressive strength and dynamic modulus of elasticity of the mortars (REF - Reference mortar; M - Raw mining residues mortars; ME - Electrodialytic treated mining residues mortars).

As expected, all the mechanical properties decreased when cement was replaced by mining residues, in a proportional way. This is explained by the cement content decrease and its replacement by the residues that are lower strength materials (as shown in Table 1). The non-pozzolanic behaviour of these residues may also justify the decrease observed in mechanical properties. Raw mining residues reported only 8 mg of $Ca(OH)_2$ fixation and ED mining residues 71 mg (Almeida et al., 2020c), being both samples far below the limit (660 mg $Ca(OH)_2/g$) to be considered as pozzolans according to NF P 18-513 (AFNOR, 2010).

When 10 % of raw mining residues replaced CEM II/BL 32.5 N, the loss in DME when compared to the reference was 12 %. DME translates mortars stiffness, where lower values indicate that mortars are more prone to absorb deformations (Gomes et al., 2018). Therefore, low DME may be beneficial to mortars, without jeopardizing other mechanical properties. Considering rendering and plastering mortars, cracking issues due to loading applications can be alleviated in the presence of low DME mortars (Sandin, 1995).

As expected, DME decrease is consistent with the reduction on flexural and compressive strengths. Generally, the cement replacement by mining residues provided mortars with lower strengths, which in the present circumstance was more evident in the compressive strength case. Apart the declining trend with the increase of mining residues content, that may be explained by the lower proportion of cement, a retarding effect on cement hydration can be caused by amounts of phosphorus (Jiang et al., 2019) and the presence of other chemical impurities on mining residues (Tiwari et al., 2014).

The presence of phosphorus in mining residues, as reported in Table 2 for M (0.15 %) and ME mortars (0.10 %), may have contributed to decrease mechanical performance. Internal micro-cracking of mortars may also have occurred, although this behaviour is more common in the presence of high cement contents (Gomes et al., 2018).

Comparing to the reference, mechanical strength decreased 11 % and 19 % in terms of flexural performance in M10 and ME10, respectively. Also, for the same formulations a decrease of 30 % on compressive strength occurred. Other studies conducted aiming mortars production with blended cements including mining waste also reported a decrease in compressive and flexural strengths, that becomes more pronounced as the mining waste content increases (Caneda-Martínez et al., 2019, 2018; Choi et al., 2009; Wu et al., 2020).

Additionally, mortars that couple resistance to cracking and deformability can be evaluated by DME/flexural strength ratio, where low values mean increased mechanical performance. Thus, M and ME mortars showed better DME/flexural strength ratio in the following sequence:

M50 > M25 > ME25 > ME10 > ME50 > REF > M10.

3.3.3. Mortars classification and application

Renders and masonry joint repointing mortars, as highly exposed construction elements, need to be repaired and eventually replaced cyclically during buildings life cycle (Sandin, 1995). Considering the classification for rendering (and plastering) mortars from EN 998-1 (CEN, 2016a), mortars with mining residues may be classified according to their compressive

strength at 28 days as CS III (M25, ME25, M50 and ME50) and CS IV (M10 and ME10). These classes are much superior to the limit for CS I mortars (0.4 MPa), corresponding to extremely stiff mortars to some traditional and historical walls. Therefore, even the mortars with 50 % of cement replace by mining residues presented mechanical performances compatible with common concrete and contemporary fired brick masonry walls.

On the other hand, regarding EN 998-2 (CEN, 2016b) classification of bedding mortars for masonry units layering, mortars with mining residues can be classified in classes M5 (M50 and ME50) and M10 (M10, ME10, M25 and ME25). Concerning class M1 (maximum of 1 MPa), the mortars produced are not in compliance with some traditional and historical walls low resistance needs. As the previous case, M50 also showed compatibility with traditional concrete and contemporary fired brick masonry walls.

Furthermore, the incorporation of 10 and 50 % of mining residues after the ED treatment was not significantly affected, in comparison to the raw mining residues use, considering applications where compressive strength is essential. Contrarily, when flexural strength is the key factor, such as for rendering, plastering and joint repointing, mortars with both 10 % and 25 % of ED mining residues showed better properties in comparison to the replacement of cement by raw mining residues. In addition, the mechanical performance of ME mortars was not strongly affected when compared to M mortars.

3.3.4. Water absorption by capillarity and drying

The capillarity curves allow to evaluate the initial absorption rate of mortars, by the capillary coefficient, and the total absorbed water, by the asymptotic value. The average capillarity curves of mortars are presented in Figure 6.

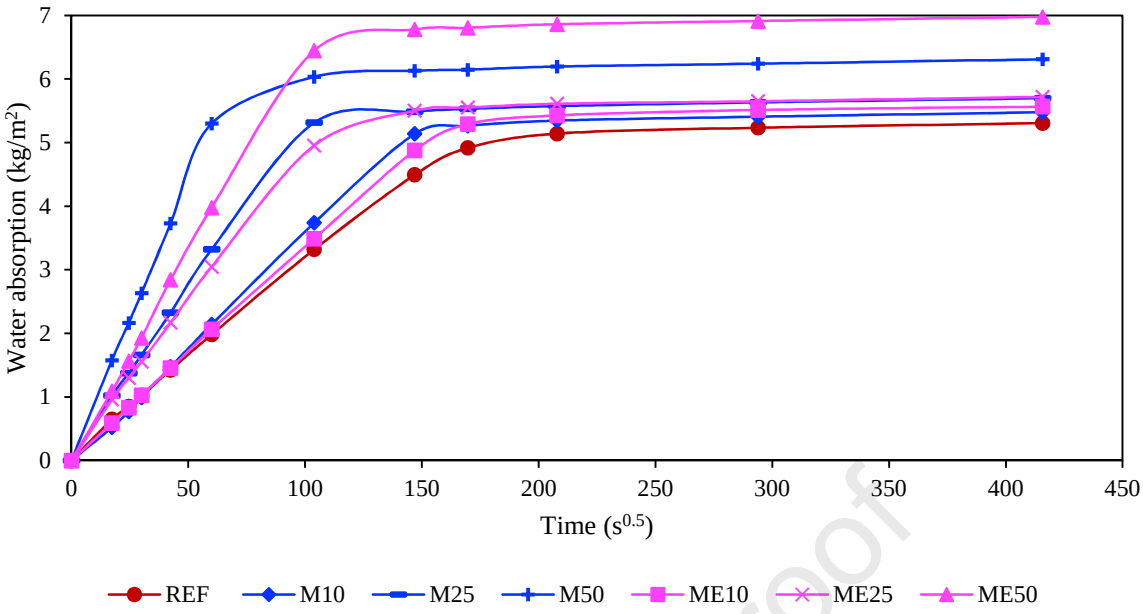

Figure 6. Capillarity absorption curves of mortars (REF - Reference mortar; M - Raw mining residues mortars; ME - Electrodialytic treated mining residues mortars).

The capillary curves showed that all the mortars with mining residues behaved negatively in comparison to REF in terms of capillary absorption, proportionally to the residue increase. Mortars with 10 % of mining residues presented similar values both in terms of initial capillarity absorption rate and asymptotic value. Mortars with 25 % of residues, although presented an increase of initial absorption rate, maintained an equivalent total of water absorbed by capillarity. Mortars with 50 % residues not only showed an increase on the initial rate but also on the total absorbed water, that may be explained by the mortars pore size distribution. The initial absorption rate is quantified by the capillarity coefficient in Table 4, as well as capillarity saturation values.

Table 4. Capillarity absorption coefficient, capillarity saturation value, drying rates of phases 1 and 2 and drying index of mortars.

Mortar	Cac [kg/(m^2.s$^{0.5}$)]	Cs (kg/m^2)	DR$_1$ [kg/(m^2.h)]	DR$_2$ [kg/(m^2.h$^{0.5}$)]	Drying index
REF	0.033 ± 0.001	5.305 ± 0.593	0.204 ± 0.003	0.456 ± 0.002	0.216 ± 0.009
M10	0.035 ± 0.000	5.476 ± 0.140	0.195 ± 0.010	0.472 ± 0.007	0.218 ± 0.011
M25	0.055 ± 0.002	5.698 ± 0.685	0.192 ± 0.009	0.501 ± 0.008	0.220 ± 0.001
M50	0.088 ± 0.000	6.309 ± 0.337	0.218 ± 0.011	0.594 ± 0.011	0.197 ± 0.000
ME10	0.034 ± 0.000	5.564 ± 0.041	0.206 ± 0.011	0.444 ± 0.006	0.257 ± 0.000
ME25	0.051 ± 0.000	5.717 ± 0.742	0.200 ± 0.019	0.507 ± 0.016	0.228 ± 0.000
ME50	0.067 ± 0.005	6.976 ± 0.198	0.221 ± 0.007	0.539 ± 0.004	0.284 ± 0.001

Notation: REF - Reference mortar; M - Raw mining residues mortars; ME - Electrodialytic treated mining residues mortars; Cac - Capillarity absorption coefficient; Cs - Capillarity saturation value; DR$_1$ - Drying rate (phase 1); DR$_2$ - Drying rate (phase 2).

From the observation of the capillary curves (Figure 6 and Table 4), the capillarity coefficient increased with the increase of mining residues incorporation, as well as the capillarity saturation value. Additionally, no significant deterioration on those properties occurred between mortars with raw or ED mining residues, being the ED case more advantageous for the product lifecycle.

Capillarity coefficients of M50 [0.088 ± 0.000 kg/(m^2.$s^{0.5}$)] and ME50 [0.067 ± 0.005 kg/(m^2.$s^{0.5}$)] represented the worst cases, since these formulations absorbed water faster and in higher quantities (6.309 ± 0.337 kg/m^2 and 6.976 ± 0.198 kg/m^2 , respectively). On the other hand, M10 and ME10 presented a behaviour similar to REF [0.03 kg/(m^2.$s^{0.5}$)], probably due to their identical permeability properties. Capillarity saturation values and higher rates of initial water absorption compared to the reference mortar were also observed in cement mortars with copper mine tailings incorporation (Onuaguluchi and Eren, 2012).

Mortars water absorption may also have been affected by the internal cure of mortar samples, since mining residues particles may had retained more water in comparison to cement. Thus, short term cement hydration could have hindered, changing porous structure (Corinaldesi, 2009; Simonsen et al., 2020).

Concerning durability issues, the presence of water accelerates the degradation of mortars, as the entry of harmful agents and salts solubilization is facilitated. High drying rates are a key factor for preventing mortars deterioration, given that the drying difficulty of a saturated material may also potentiate the growth of fungi and algae (Salomão et al., 2018).

Following water absorption by capillarity experiments, drying tests were carried out with the same mortar samples. Figure 7 shows the drying curves of the mortars as function of time and of square root of time.

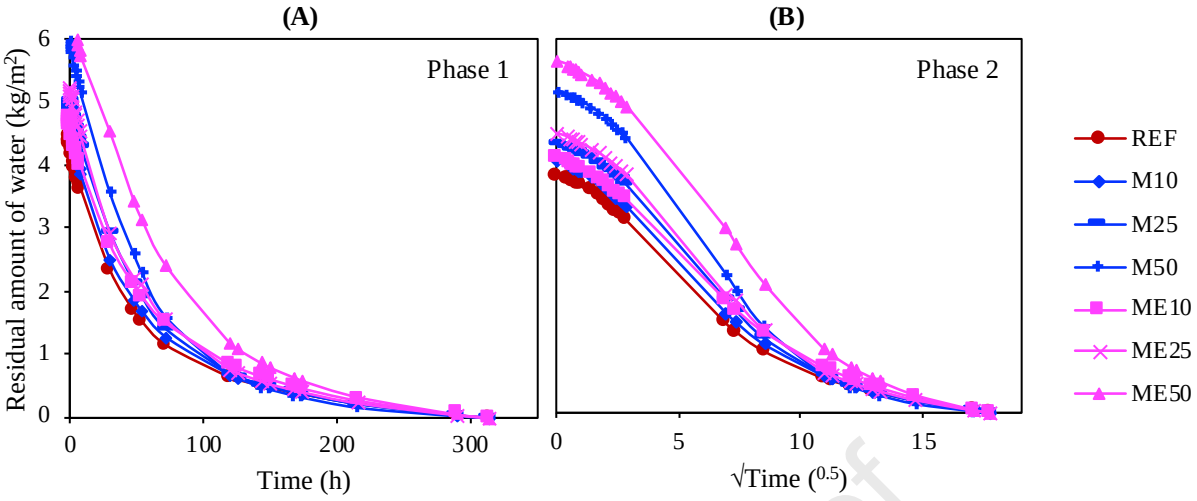

Figure 7. Drying curves of mortars: (A) by time, showing the initial slope of drying phase 1; (B) by square root of time, showing the intermediate slope of drying phase 2 (REF - Reference mortar; M - Raw mining residues mortars; ME - Electrodialytic treated mining residues mortars).

The drying rates in both phases 1 and 2 are presented in Table 4. The drying rate for phase 1, DR_1, was about 0.2 kg/(m^2.h) for all the tested mortars, although the lowest absolute values were observed for M25 and ME25, and the highest for M50 and ME50.

The drying rate obtained for phase 2, DR_2, was also higher for mortars with 50 % of mining residues incorporation, confirming that the binder matrix is important for water release through the mortars pores. Mortars with mining residues generally presented an increase in the evaporation rate as a consequence of the improved diffusion and permeability.

The results showed that M10 and ME10 obtained the best performance compared to the other modified mortars. Hence, the incorporation percentage of mining residues can influence mortars' drying capacity. Additionally, during the drying process, the presence of soluble salts may promote its crystallization at the sample surface, giving rise to efflorescence or leaching inert materials into the pores causing staining (Faria et al., 2008). In the studied mortars samples, no salt crystallization was observed during drying. Concerning mortars´ drying rates, the use of ED mining residues is promising in comparison to both raw mining residues and reference mortars.

Drying index was determined to understand the overall behaviour of the mortars drying (Table 4). The lower drying index was found for M50 (0.197 ± 0.000), indicating that mortars with raw mining residues can dry easier. M50 absorbed water quickly and achieved a moisture content higher than other formulations. However, these mortars dried easily and, at

the end of drying, the content of residual water in the pores was lower than for the other samples.

ME10, ME25 and ME50 showed lower capacity to completely dry (corroborated by their higher drying index). These mortars required exposure to a high-intensity source of moisture for a long period to completely saturate. After saturation, the material dried out more hardly, remaining humid for a longer time and keeping a higher moisture content in pores compared to the other formulations.

The behaviour of the mortars during the drying process can be related to their water absorption, as the drying process includes transport mechanisms of water (Salomão et al., 2018). The higher the absorbed water content, the faster the transport velocity of water to the surface where evaporation occurs in the first drying phase.

3.3.5. Porosity and porosimetry of mortars

Due to capillarity absorption similar results considering mortars with the same content of raw and ED mining residues, mercury intrusion porosimetry (MIP) analysis was only performed to compare REF and M mortars. Through MIP, open porosity of mortars was reported higher in sequence M10 (21.01 %) ≤ M25 (21.70 %) ≤ REF (22.05 %) < M50 (30.76 %). M10, M25 and REF showed similar porosities, meaning that cement replacement until 25 % did not promote significant changes in open porosity. The pore size distribution of REF and M mortars is presented on Figure 8.

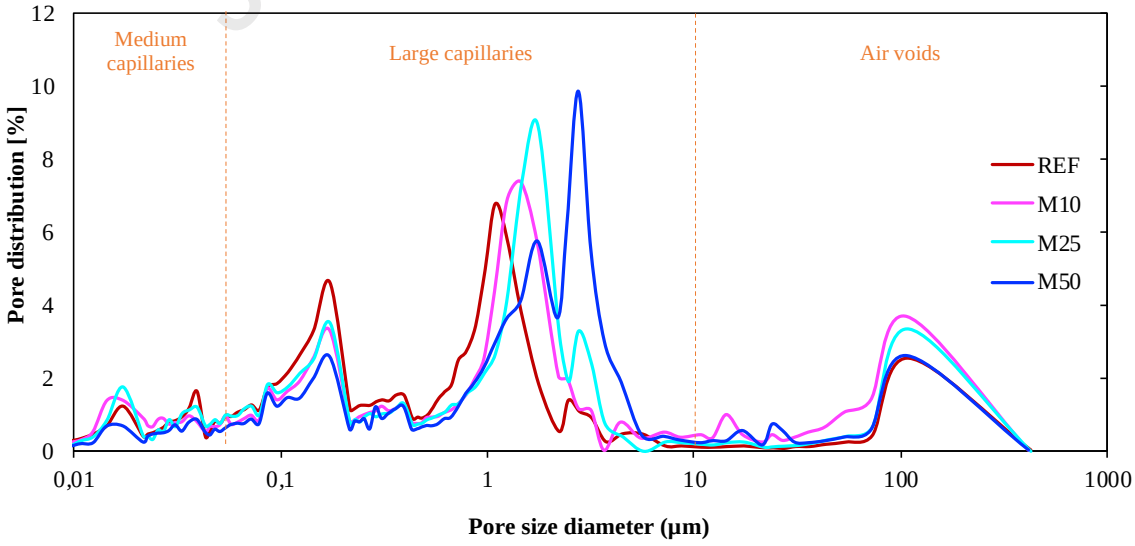

Figure 8. Pore size distribution of REF and M mortars (REF - Reference mortar; M - Raw mining residues mortars).

As presented in Figure 8, in the range of medium capillaries (large mesopores), M25 has a prevalence. REF is dominant on the low range of large capillary pores (macropores), with ~~a~~ peaks at 0.17 μm and 0.40 μm. A higher amount of cement in mortar composition leads to an increase of volume in this porosity range, attributed to the clinker phase (Santos et al., 2020). Other authors reported the same trend (Arizzi and Cultrone, 2013), which may also be justified by a higher water retention by the mortars with mining residues during short term hydration.

Regarding large capillary pores, above 1 μm, there is a pore size diameter gradual increase, as well as its concentration, from mortars with 0 % (REF = 1.1 μm / 6.8 %) to 50 % (M50 = 2.8 μm / 9.9 %) of cement replacement by raw residues. The large capillary pores distribution can be affected by the binder-aggregate interaction. When low cement contents were used, the formation of hydration products that improve hydration and carbonation reactions at early ages could be affected, influencing packing density and consequently pores distribution (Santos et al., 2020). In the range of air voids, there is a prevalence on M10 mortar.

The trend on capillary water absorption may be justified by the increased porosimetry of mortars with increased residue content in the range of 1 to 6 μm. The highest porosimetry of M50 corroborates the increase of capillary water absorption.

Mortars with mining residues generally presented an increase in the evaporation rate due to their higher capillary and total porosity and pore diameter, in comparison with the reference mortar. Also, low drying index values are associated to a higher large capillary porosity of mortars (Santos et al., 2020).

The low level of mortar compactness, as well as air/liquid losses, may influence strength and durability properties, although it could be advantageous in terms of freeze-thaw and salt decay (Santos et al., 2018). An increase of volume and diameter pore size of the coarse porosity promoted a decrease on mechanical performance, namely in compressive strength (Figure 5), and an increase of water absorption by capillarity (Figure 6) and the drying capacity (Figure 7). This trend was also observed in cement-mortars studies performed by Santos et al. (2020).

4. Conclusions

Resource efficiency regarding the decrease of residues generation and disposal is an important step towards a cleaner production in the construction and mining industries. Cement clinker production requires firing temperatures above 1000 ºC and energy-consuming milling. When cement is partially replaced by mining residues for mortars production,

environmental and economic advantages can be achieved, ensuring economic circularity and increasing the added value of mining secondary resources.

Furthermore, the recovery of critical raw materials and the removal of harmful compounds from those residues is also an important challenge. Therefore, an electrodialytic (ED) process was applied to Panasqueira mining residues to recover tungsten and remove arsenic in a first stage.

The effect of the ED treatment on mortars properties was address through the study of mortars performance, when compared to the same contents of raw mining residues and a reference cement binder mortar. Mortars were produced using 0, 10, 25 and 50 % of mining residues replacing cement, maintaining the water/binder ratio (0.5) for 1:3 volumetric proportion of binder:river sand mortars, where the binder was the sum of cement and residues.

Mining residues seemed to have permeability and surface properties that imply the requirement of higher amounts of water to achieve the same consistency, as when using only cement. Thus, further studies should be conducted with different water contents to access the influence on mortars properties versus types of applications. Also, to tackle water scarcity, the reuse of secondary liquid matrices to replace water applications may also be a key factor towards a more sustainable mortar production.

Mechanical performance decreased between 11 and 30 %, when 10 % of mining residues were incorporated in the formulation. As expected, this decrease was more pronounced with the increasing of mining residues content replacing cement. On the other hand, the increase on mining residues incorporation corresponded to an increase on capillary absorption, justified by mortars porosimetry, and that could be controlled by higher drying rates.

All tested mortars showed mechanical and physical properties suitable for rendering, plastering, joint repointing, bedding masonry or screed uses, with improved thermal conductivity. However, to optimize mortars properties, expand the applications and increase mining residues replacement ratios, under a sustainable perspective, natural additives and admixtures (e.g. re-used oils) could also be tested.

Summing up, results showed that the ED technology could be applied as a pre-treatment for mining residues since physical and mechanical mortars' properties were not deteriorated when compared with mortars formulated with raw mining residues. The ED treatment coupled benefits from a previous removal of harmful compounds and recovery of critical raw materials, providing a more sustainable working material. Mortars produced with treated mining residues are more advantageous in terms of toxicity and, considering the overall

product lifecycle, can alleviate the negative impacts associated to their production, when compared to pure cement or cement-raw residues mortars.

Acknowledgments

This work has received funding from the European Union's Horizon 2020 research and innovation program under the Marie Skłodowska-Curie grant agreement No. 778045, as well as from Portuguese funds from FCT/MCTES through grant UIDB/04085/2020. J. Almeida acknowledges *Fundação para a Ciência e a Tecnologia* and EcoCoRe Doctoral program for her PhD fellowship PD/BD/135170/2017. The authors acknowledge Eng. Manuel Pacheco from Panasqueira mine for providing mining residues samples and Eng. Vítor Silva for assistance during mortar formulation and mechanical tests.

References

AFNOR, 2010. NF P 18-513 – Métakaolin, addition pouzzolanique pour bétons - Définitions, spécifications, critères de conformité. Paris.

Almeida, J., Craveiro, R., Faria, P., Silva, A.S., Mateus, E.P., Barreiros, S., Paiva, A., Ribeiro, A.B., 2020a. Electrodialytic removal of tungsten and arsenic from secondary mine resources — Deep eutectic solvents enhancement. Sci. Total Environ. 710, 136364. https://doi.org/10.1016/j.scitotenv.2019.136364

Almeida, J., Ribeiro, A.B., Silva, A.S., Faria, P., 2020b. Overview of mining residues incorporation in construction materials and barriers for full-scale application. J. Build. Eng. 29, 101215. https://doi.org/10.1016/j.jobe.2020.101215

Almeida, J., Santos Silva, A., Faria, P., Ribeiro, A., 2020c. Assessment on tungsten mining residues potential as partial cement replacement. KnE Eng. 5, 228–237. https://doi.org/10.18502/keg.v5i4.6814

Arizzi, A., Cultrone, G., 2013. The influence of aggregate texture, morphology and grading on the carbonation of non-hydraulic (aerial) limebased mortars. Q. J. Eng. Geol. Hydrogeol. 46, 507–520. https://doi.org/10.1144/qjegh2012-017

Arrigoni, A., Panesar, D.K., Duhamel, M., Opher, T., Saxe, S., Posen, I.D., MacLean, H.L., 2020. Life cycle greenhouse gas emissions of concrete containing supplementary cementitious materials: cut-off vs. substitution. J. Clean. Prod. 263, 121465.

https://doi.org/10.1016/j.jclepro.2020.121465

Beghoura, I., Castro-Gomes, J., 2019. Design of alkali-activated aluminium powder foamed materials for precursors with different particle sizes. Constr. Build. Mater. 224, 682–690. https://doi.org/10.1016/j.conbuildmat.2019.07.018

Brás, A., Faria, P., 2017. Effectiveness of mortars composition on the embodied carbon long-term impact. Energy Build. 154, 523–528. https://doi.org/10.1016/j.enbuild.2017.08.026

Caneda-Martínez, L., Frías, M., Medina, C., de Rojas, M.I.S., Rebolledo, N., Sánchez, J., 2018. Evaluation of chloride transport in blended cement mortars containing coal mining waste. Constr. Build. Mater. 190, 200–210. https://doi.org/10.1016/j.conbuildmat.2018.09.158

Caneda-Martínez, L., Medina, C., Sánchez de Rojas, M.I., Frías, M., 2019. Water transport in binary eco-cements containing coal mining waste. Cem. Concr. Compos. 104, 103373. https://doi.org/10.1016/j.cemconcomp.2019.103373

Capasso, I., Lirer, S., Flora, A., Ferone, C., Cioffi, R., Caputo, D., Liguori, B., 2019. Reuse of mining waste as aggregates in fly ash-based geopolymers. J. Clean. Prod. 220, 65–73. https://doi.org/10.1016/j.jclepro.2019.02.164

Castro-Gomes, J.P., Silva, A., Cano, R.P., Durán Suarez, A., 2011. Recycled materials for technical-artistic applications obtained with tungsten mine coarse wastes, in: International Conference on Sustainability of Constructions - Towards a Better Built Environment. Innsbruck.

Castro-Gomes, J.P., Silva, A.P., Cano, R.P., Durán Suarez, J., Albuquerque, A., 2012. Potential for reuse of tungsten mining waste-rock in technical-artistic value added products. J. Clean. Prod. 25, 34–41. https://doi.org/10.1016/j.jclepro.2011.11.064

CEN, 2019. EN 1015-11:2019 - Methods of test for mortar for masonry. Part 11: Determination of flexural and compressive strength of hardened mortar. Belgium.

CEN, 2017. EN 196-1: 2017 - Methods of testing cement. Part 1: Determination of strength. Belgium.

CEN, 2016a. EN 998-1:2016 - Specification for mortar for masonry. Part 1: Rendering and

plastering mortar.

CEN, 2016b. EN 998-2:2016 - Specification for mortar for masonry. Part 2: Masonry mortar.

CEN, 2013. EN 16322:2013 - Conservation of cultural heritage. Test methods. Determination of drying properties. Belgium.

CEN, 2012. EN 197-1:2012 - Cement. Part 1: Composition, specifications and conformity criteria for common cements. Belgium.

CEN, 2004. EN 14146:2004 - Natural stone test methods - Determination of the dynamic modulus of elasticity (by measuring the fundamental resonance frequency). Belgium.

CEN, 2003. EN 1015-18:2003 - Methods of test for mortar for masonry. Part 18: Determination of water absorption coefficient due to capillary action of hardened mortar. Belgium.

CEN, 2000. EN 1015-3:2000 - Methods of test for mortars for masonry. Part 3: Determination of consistence of fresh mortars (by Flow Table). Belgium.

CEN, 1999a. EN 1015-6:1999 Methods of test for mortar for masonry. Part 6: Determination of bulk density of fresh mortar. Belgium.

CEN, 1999b. EN 1015-10:1999/A1:2006 - Methods of test for mortar for masonry. Part 10: Determination of dry bulk density of hardened mortar. Belgium.

CEN, 1998. EN 1015-1:1998 - Methods of test for mortar for masonry. Part 1: Determination of particle size distribution (by sieve analysis). Belgium.

Chindaprasirt, P., Cao, T., 2015. Setting, segregation and bleeding of alkali-activated cement, mortar and concrete binders, in: Handbook of Alkali-Activated Cements, Mortars and Concretes. Elsevier Inc., pp. 113–131. https://doi.org/10.1533/9781782422884.2.113

Choi, Y.W., Kim, Y.J., Choi, O., Lee, K.M., Lachemi, M., 2009. Utilization of tailings from tungsten mine waste as a substitution material for cement. Constr. Build. Mater. 23, 2481–2486. https://doi.org/10.1016/j.conbuildmat.2009.02.006

Corinaldesi, V., 2009. Mechanical behavior of masonry assemblages manufactured with recycled-aggregate mortars. Cem. Concr. Compos. 31, 505–510.

https://doi.org/10.1016/j.cemconcomp.2009.05.003

Di Mundo, R., Seara-Paz, S., González-Fonteboa, B., Notarnicola, M., 2020. Masonry and render mortars with tyre rubber as aggregate: Fresh state rheology and hardened state performances. Constr. Build. Mater. 245, 118359. https://doi.org/10.1016/j.conbuildmat.2020.118359

EC, 2020. Communication from the Comission to the European Parliament,the Council, the European Economic and Social Comittee and the Comittee of the Regions - A new Circular Economy Action Plan for a cleaner and more competitive Europe. Brussels.

Faria, P., Dias, I., Jamú, N., Silva, V., 2015. Air lime-earth blended mortars - Assessment on fresh state and workability, in: International Conference on Vernacular Heritage, Sustainability and Earthen Architecture.

Faria, P., Henriques, F., Rato, V., 2008. Comparative evaluation of lime mortars for architectural conservation. J. Cult. Herit. 9, 338–346. https://doi.org/10.1016/j.culher.2008.03.003

Franco, A., Vieira, R., Bunting, R., 2014. The Panasqueira mine at a glance, Tungsten. International Tungsten Industry Association.

Gankhuyag, U., Gregoire, F., 2018. Managing mining for sustainable development. A sourcebook. Bangkok: United Nations Development Programme.

Gomes, M.I., Faria, P., Gonçalves, T.D., 2018. Earth-based mortars for repair and protection of rammed earth walls. Stabilization with mineral binders and fibers. J. Clean. Prod. 172, 2401–2414. https://doi.org/10.1016/j.jclepro.2017.11.170

Guedes, P., Mateus, E., Almeida, J., Ferreira, A., Couto, N., Ribeiro, A., 2016. Electrodialytic treatment of sewage sludge: current intensity influence on phosphorus recovery and organic contaminants removal. Chem. Eng. J. 306, 1058–1066. https://doi.org/10.1016/j.cej.2016.08.040

Guedes, P., Mateus, E.P., Couto, N., Rodríguez, Y., Ribeiro, A.B., 2014. Electrokinetic remediation of six emerging organic contaminants from soil. Chemosphere 117C, 124–131. https://doi.org/10.1016/j.chemosphere.2014.06.017

Jesus, S., Maia, C., Brazão Farinha, C., de Brito, J., Veiga, R., 2019. Rendering mortars with incorporation of very fine aggregates from construction and demolition waste. Constr. Build. Mater. 229, 116844. https://doi.org/10.1016/j.conbuildmat.2019.116844

Jiang, Y., Ling, T.C., Mo, K.H., Shi, C., 2019. A critical review of waste glass powder – Multiple roles of utilization in cement-based materials and construction products. J. Environ. Manage. https://doi.org/10.1016/j.jenvman.2019.04.098

Lèbre, É., Corder, G.D., Golev, A., 2017. Sustainable practices in the management of mining waste: A focus on the mineral resource. Miner. Eng. 107, 34–42. https://doi.org/10.1016/j.mineng.2016.12.004

Li, L., Liu, W., You, Q., Chen, M., Zeng, Q., 2020. Waste ceramic powder as a pozzolanic supplementary filler of cement for developing sustainable building materials. J. Clean. Prod. 259, 120853. https://doi.org/10.1016/j.jclepro.2020.120853

Magro, C., Paz-Garcia, J.M., Ottosen, L.M., Mateus, E.P., Ribeiro, A.B., 2019. Sustainability of construction materials: Electrodialytic technology as a tool for mortars production. J. Hazard. Mater. 363, 421–427. https://doi.org/10.1016/j.jhazmat.2018.10.010

Magro, C.C., Guedes, P.R., Kirkelund, G.M., Jensen, P.E., Ottosen, L.M., Ribeiro, Alexandra B., 2016. Incorporation of different fly ashes from mswi as substitute for cement in mortar: an overview of the suitability of electrodialytic pre-treatment, in: Ribeiro, A.B., Mateus, E.P., Couto, N. (Eds.), Electrokinetics Across Disciplines and Continents. Springer International Publishing, Cham, pp. 225–247. https://doi.org/10.1007/978-3-319-20179-5_12

Onuaguluchi, O., Eren, Ö., 2012. Recycling of copper tailings as an additive in cement mortars. Constr. Build. Mater. 37, 723–727. https://doi.org/10.1016/j.conbuildmat.2012.08.009

Palomar, I., Barluenga, G., Ball, R.J., Lawrence, M., 2019. Laboratory characterization of brick walls rendered with a pervious lime-cement mortar. J. Build. Eng. 23, 241–249. https://doi.org/10.1016/j.jobe.2019.02.001

Ribeiro, A.B., Mateus, E.P., Ottosen, L.M., Bech-Nielsen, G., 2000. Electrodialytic removal of Cu, Cr, and As from chromated copper arsenate-treated timber waste. Environ. Sci.

Technol. 34, 784–788. https://doi.org/10.1021/es990442e

Ribeiro, A.B., Rodríguez-Maroto, J.M., 2006. Electroremediation of heavy metal-contaminated soils -processes and applications, in: Prasad, M.N.V., Sajwan, K.S., Naidu, R. (Eds.), Trace Elements in the Environment: Biogeochemistry, Biotechnology, and Bioremediation. CRC Press, Florida, USA, pp. 341–368. https://doi.org/http://dx.doi.org/10.1385/BTER:109:3:301

Salomão, M.C. de F., Bauer, E., Kazmierczak, C. de S., 2018. Drying parameters of rendering mortars. Ambient. Construído 18, 7–19. https://doi.org/10.1590/s1678-86212018000200239

Sandin, K., 1995. Mortars for Masonry and Rendering Choice and Application. Build. Issues 7.

Santos, A.R., Veiga, M. do R., Santos Silva, A., de Brito, J., Álvarez, J.I., 2018. Evolution of the microstructure of lime based mortars and influence on the mechanical behaviour: The role of the aggregates. Constr. Build. Mater. 187, 907–922. https://doi.org/10.1016/j.conbuildmat.2018.07.223

Santos, A.R., Veiga, M. do R., Silva, A.S., de Brito, J., 2020. Microstructure as a critical factor of cement mortars' behaviour: The effect of aggregates' properties. Cem. Concr. Compos. 111, 103628. https://doi.org/10.1016/j.cemconcomp.2020.103628

Sedira, N., Castro-Gomes, J., Magrinho, M., 2018. Red clay brick and tungsten mining waste-based alkali-activated binder: Microstructural and mechanical properties. Constr. Build. Mater. 190, 1034–1048. https://doi.org/10.1016/j.conbuildmat.2018.09.153

Shi, J., Liu, B., Qin, J., Jiang, J., Wu, X., Tan, J., 2020. Experimental study of performance of repair mortar: Evaluation of in-situ tests and correlation analysis. J. Build. Eng. 31, 101325. https://doi.org/10.1016/j.jobe.2020.101325

Simonsen, A.M.T., Solismaa, S., Hansen, H.K., Jensen, P.E., 2020. Evaluation of mine tailings' potential as supplementary cementitious materials based on chemical, mineralogical and physical characteristics. Waste Manag. 102, 710–721. https://doi.org/10.1016/j.wasman.2019.11.037

Sousa, S., Silva, A.S., Velosa, A., Gameiro, A., Rocha, F., 2013. Mitigation of internal expansive reaction: The role of tungsten mine sludge, in: Materials Science Forum. Trans Tech Publications Ltd, pp. 468–473. https://doi.org/10.4028/www.scientific.net/MSF.730-732.468

Tiwari, P., Chandak, R., Yadav, R.K., 2014. Effect of salt water on compressive strength of concrete. J. Eng. Res. Appl. 4, 38–42.

United Nations, 2019. World population prospects 2019 highlights. New York.

Van Riessen, A., Rickard, W., Sanjayan, J., 2009. Thermal properties of geopolymers, in: Geopolymers: Structures, Processing, Properties and Industrial Applications. Elsevier Ltd., pp. 315–342. https://doi.org/10.1533/9781845696382.2.315

Wu, C.R., Hong, Z.Q., Yin, Y.H., Kou, S.C., 2020. Mechanical activated waste magnetite tailing as pozzolanic material substitute for cement in the preparation of cement products. Constr. Build. Mater. 252, 119129. https://doi.org/10.1016/j.conbuildmat.2020.119129

Table 1. Weight proportion of binder, aggregate and water used in the mortar formulations, materials loose bulk density and water/binder mass ratio.

	Binder and mining residues					**Aggregate**		**Water**		**Mass proportion**	
	CEM II/BL 32.5 N (1000 kg/m^3)		Mining residues			Sand (1540 kg/m^3)		Tap water (1000 kg/m^3)		Binder:sand :water	Cement:residue:sand
Code	%	Weight (g)	Treatment	%	Weight (g)	%	Weight (g)	%	Weight (g)		
REF	100	431.8	-	-	-					1:4.6:0.8	1:0:4.6
M10	90	388.7	No treatment (M) (1180 kg/m^3)	10	36.6					1:4.7:0.8	1:0.1:5.1
M25	75	323.9		25	91.4					1:4.8:0.8	1:0.3:6.2
M50	50	215.9		50	182.9	100	2000	100	333.3	1:5.0:0.8	1:0.9:9.3
ME10	90	388.7	Electrodialytic treated (ME) (1003 kg/m^3)	10	42.0					1:4.6:0.8	1:0.1:5.1
ME25	75	323.9		25	105.0					1:4.7:0.8	1:0.3:6.2
ME50	50	215.9		50	209.9					1:4.7:0.8	1:1.0:9.3

Notation: REF - Reference mortar; M - Raw mining residues mortars; ME – Electrodialytic treated mining residues mortars.

Table 2. Semi-quantitative chemical analysis by XRF of raw and ED mining residues (weight %).

Determinations	**Raw**	**ED**
Al_2O_3	18.80	21.98
SiO_2	68.35	65.58
P	0.15	0.10
S	0.83	0.74
Cl	N.D.	N.D.
K_2O	3.29	4.31
Ca	0.55	0.40
Ti	0.46	0.55
Mn	0.08	0.07
Fe	5.81	5.37
Cu	0.18	0.10
Zn	0.58	0.29
As	0.59	0.21
Sn	0.07	0.04
W	0.27	0.26

Notation: N.D. – Not detected.

Table 3. Mortars wet bulk density and flow table consistency.

Mortar	Flow table consistency (mm)	Wet bulk density (kg/m^3)
REF	156.3	1997.9
M10	154.3	2018.7
M25	147.8	2035.2
M50	139.5	2038.2
ME10	146.5	2029.2
ME25	132.3	2038.7
ME50	129.3	2069.8

Notation: REF - Reference mortar; M - Raw mining residues mortars; ME - Electrodialytic treated mining residues mortars.

Table 4. Capillarity absorption coefficient, capillarity saturation value, drying rates of phases 1 and 2 and drying index of mortars.

Mortar	Cac [kg/(m^2.s$^{0.5}$)]	Cs (kg/m^2)	DR_1 [kg/(m^2.h)]	DR_2 [kg/(m^2.h$^{0.5}$)]	Drying index
REF	0.033 ± 0.001	5.305 ± 0.593	0.204 ± 0.003	0.456 ± 0.002	0.216 ± 0.009
M10	0.035 ± 0.000	5.476 ± 0.140	0.195 ± 0.010	0.472 ± 0.007	0.218 ± 0.011
M25	0.055 ± 0.002	5.698 ± 0.685	0.192 ± 0.009	0.501 ± 0.008	0.220 ± 0.001
M50	0.088 ± 0.000	6.309 ± 0.337	0.218 ± 0.011	0.594 ± 0.011	0.197 ± 0.000
ME10	0.034 ± 0.000	5.564 ± 0.041	0.206 ± 0.011	0.444 ± 0.006	0.257 ± 0.000
ME25	0.051 ± 0.000	5.717 ± 0.742	0.200 ± 0.019	0.507 ± 0.016	0.228 ± 0.000
ME50	0.067 ± 0.005	6.976 ± 0.198	0.221 ± 0.007	0.539 ± 0.004	0.284 ± 0.001

Notation: REF - Reference mortar; M - Raw mining residues mortars; ME - Electrodialytic treated mining residues mortars; Cac - Capillarity absorption coefficient; Cs - Capillarity saturation value; DR_1 - Drying rate (phase 1); DR_2 - Drying rate (phase 2).

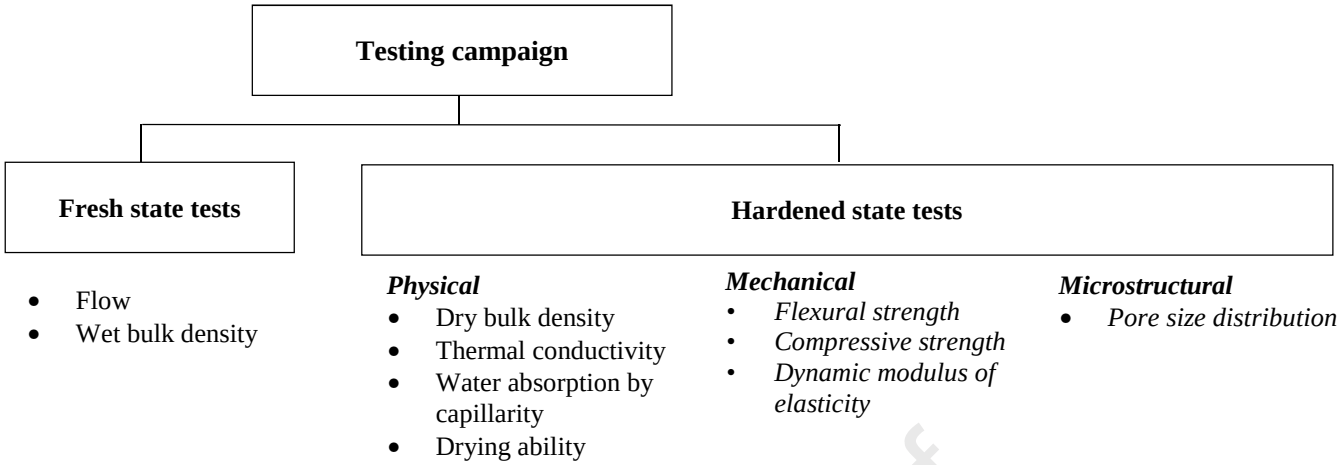

Figure 1. Tests performed to assess fresh and hardened mortars properties.

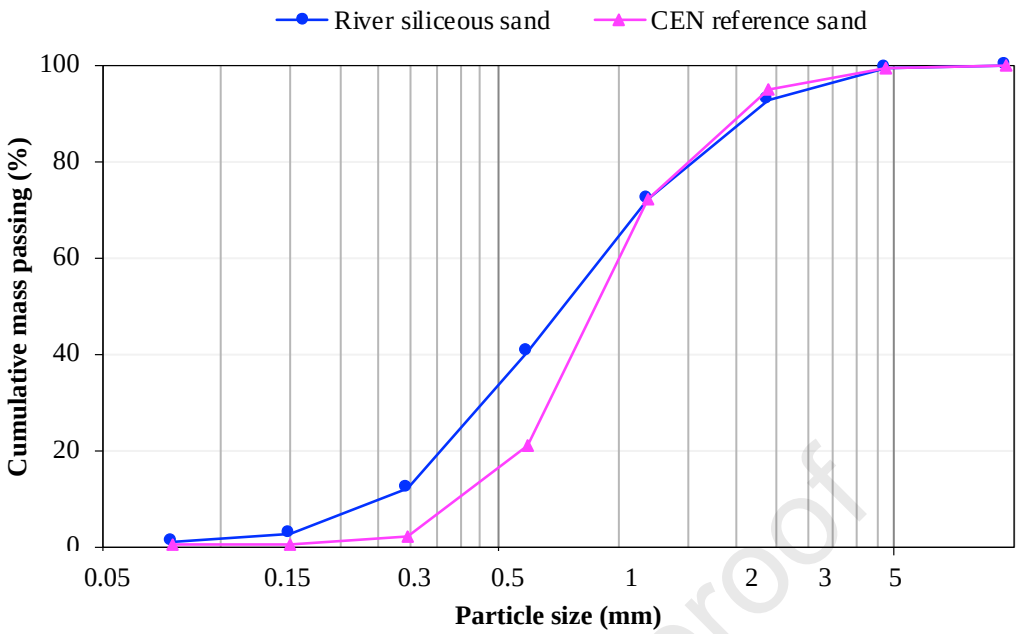

Figure 2. Dry particle size distribution of river siliceous sand and CEN reference sand.

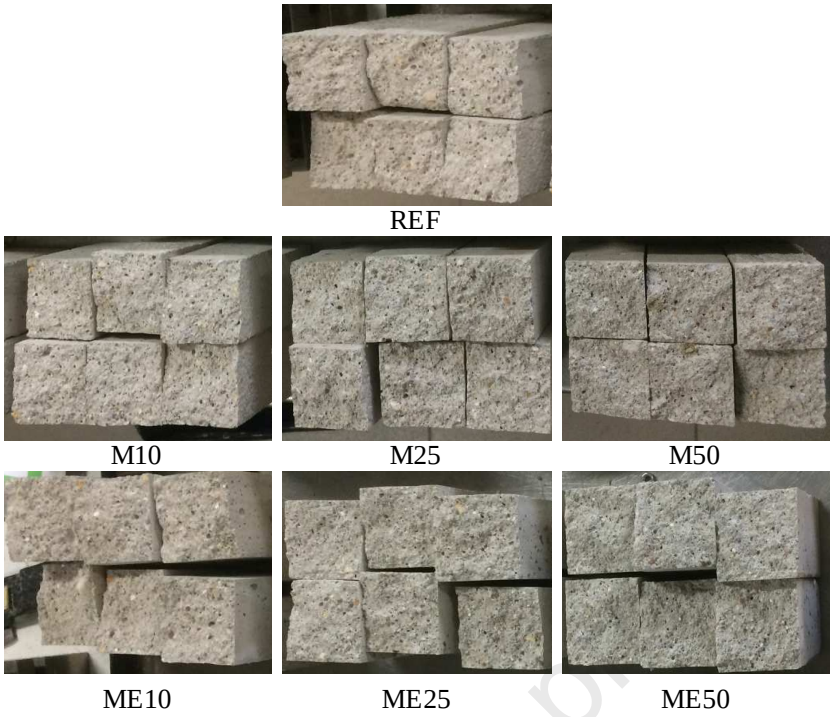

Figure 3. Mortar samples after 28 curing days (REF - Reference mortar; M - Raw mining residues mortars; ME - Electrodialytic treated mining residues mortars).

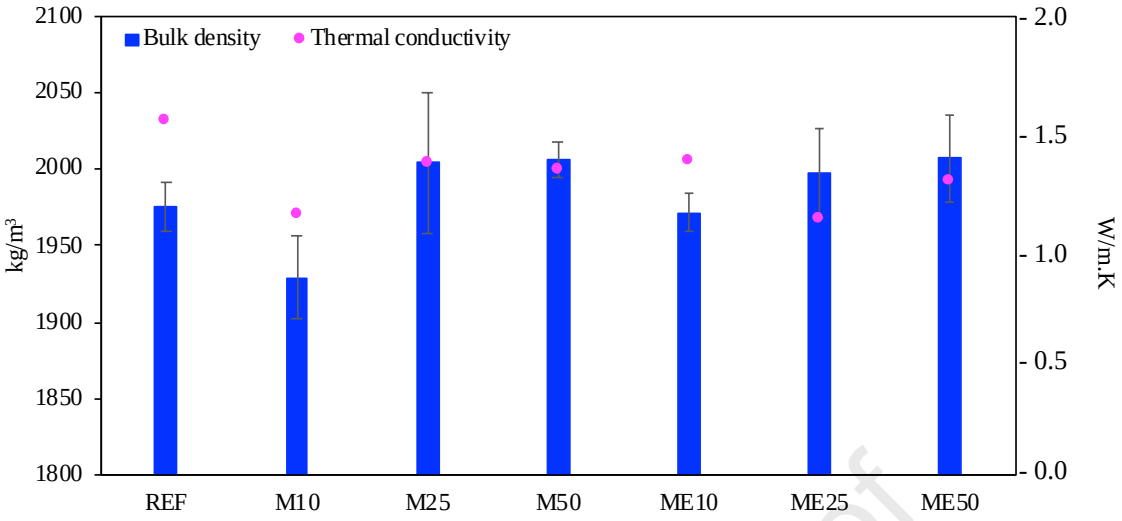

Figure 4. Dry bulk density and thermal conductivity of mortars (REF - Reference mortar; M - Raw mining residues mortars; ME - Electrodialytic treated mining residues mortars).

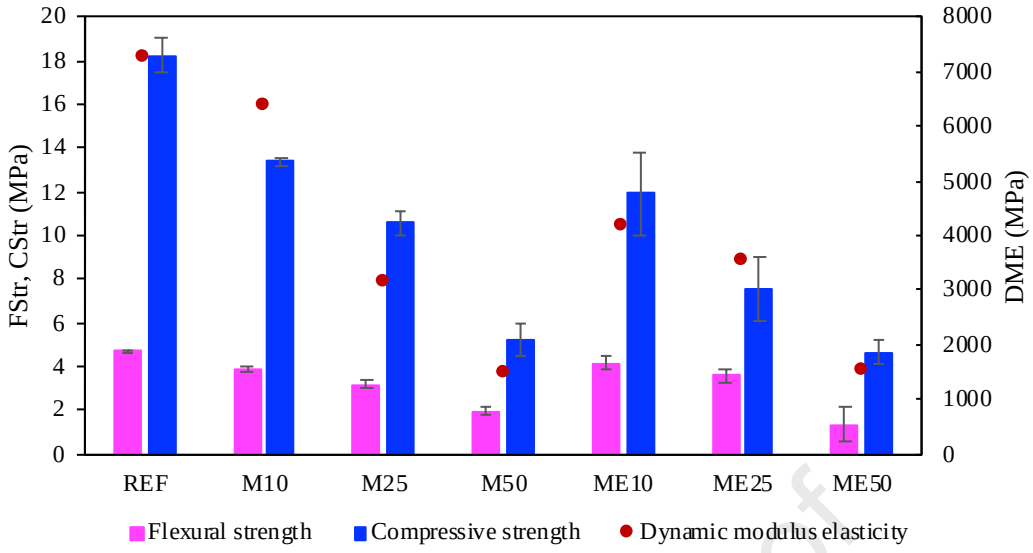

Figure 5. Flexural and compressive strength and dynamic modulus of elasticity of the mortars (REF - Reference mortar; M - Raw mining residues mortars; ME - Electrodialytic treated mining residues mortars).

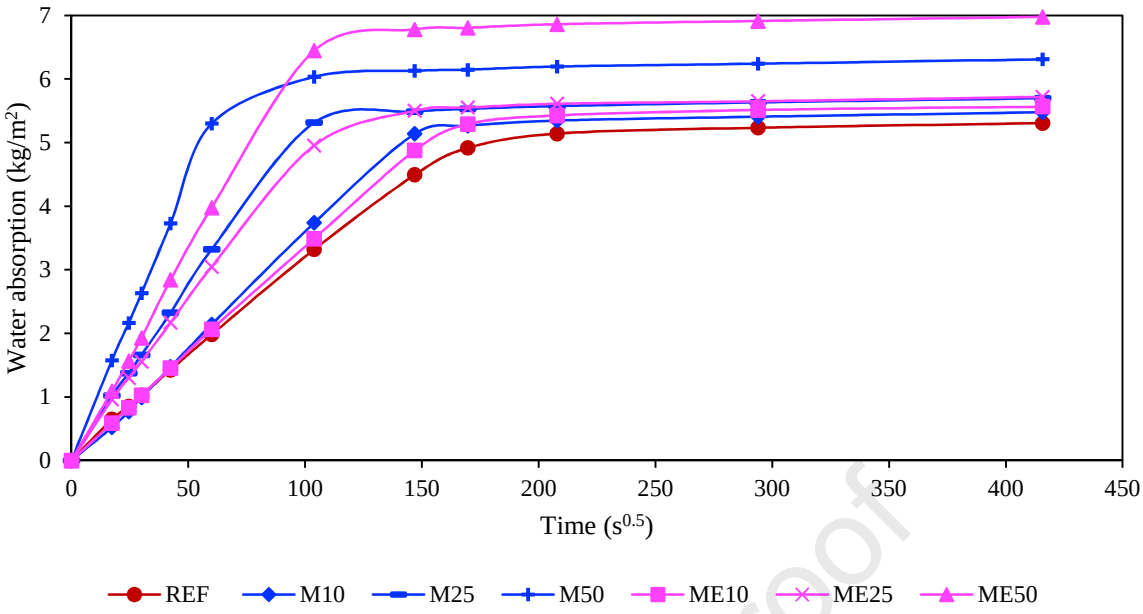

Figure 6. Capillarity absorption curves of mortars (REF - Reference mortar; M - Raw mining residues mortars; ME - Electrodialytic treated mining residues mortars).

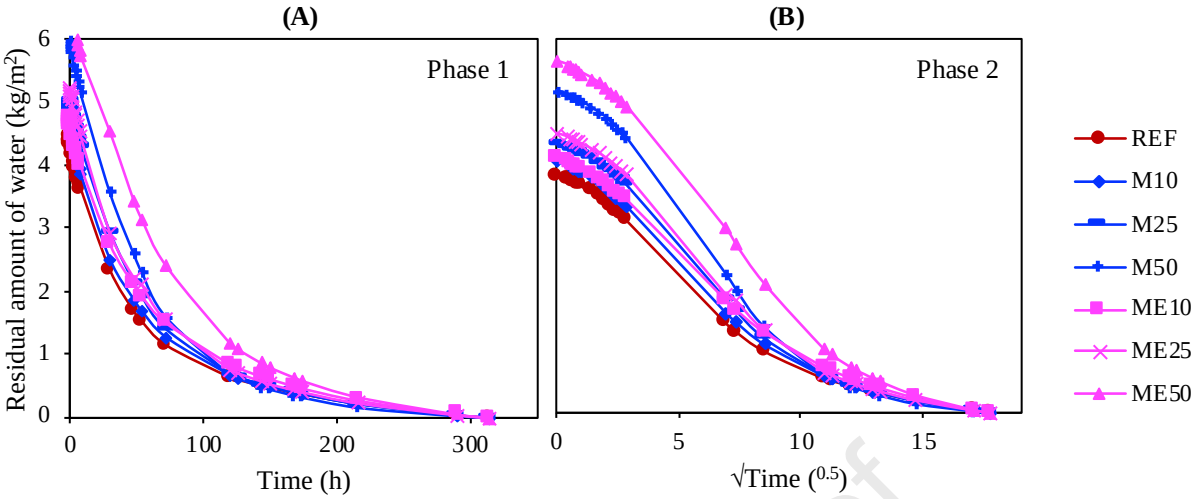

Figure 7. Drying curves of mortars: (A) by time, showing the initial slope of drying phase 1; (B) by square root of time, showing the intermediate slope of drying phase 2 (REF - Reference mortar; M - Raw mining residues mortars; ME - Electrodialytic treated mining residues mortars).

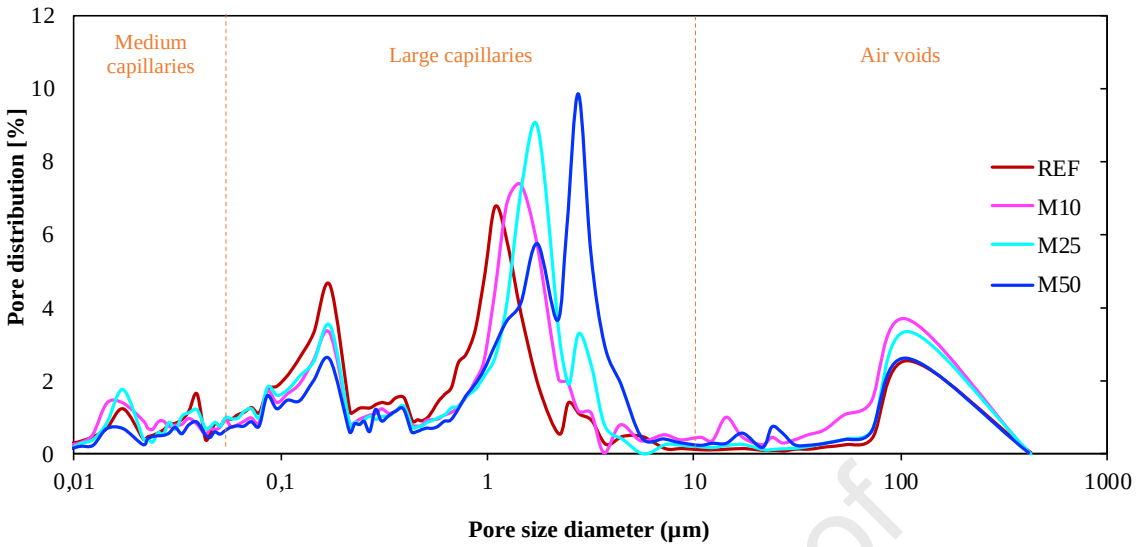

Figure 8. Pore size distribution of REF and M mortars (REF - Reference mortar; M - Raw mining residues mortars).

Highlights

- Mining residues were electrodialytic treated (ED) to extract raw materials
- Raw and ED mining residues replaced cement in 10, 25 and 50 % (volume) in mortars
- Mechanical strength of modified mortars decreased between 11 and 30 %
- Water absorption increased although drying capacity of modified mortars was improved
- ED mining residues are viable mortar materials for masonry, rendering and screeds

Declaration of interests

☒ The authors declare that they have no known competing financial interests or personal relationships that could have appeared to influence the work reported in this paper.

☐The authors declare the following financial interests/personal relationships which may be considered as potential competing interests: